



## Electrochemical properties of powder-pressed Pb–Ag–PbO<sub>2</sub> anodes

Hai-hua LI<sup>1</sup>, Tie-chui YUAN<sup>1</sup>, Rui-di LI<sup>1</sup>, Wen-jun WANG<sup>1,2</sup>, Dan ZHENG<sup>1</sup>, Ji-wei YUAN<sup>3</sup>

1. State Key Laboratory of Powder Metallurgy, Central South University, Changsha 410083, China;

2. Zhuzhou Smelter Group Company Limited, Zhuzhou 412004, China;

3. Guizhou R&D Center of Titanium Materials Co., Ltd., Zunyi 563004, China

Received 30 April 2019; accepted 21 August 2019

**Abstract:** Pb–Ag–PbO<sub>2</sub> composite anodes with different mass fractions (1%, 2%, 3%, 4% and 5%) of  $\beta$ -PbO<sub>2</sub> were prepared by powder-pressed (PP) method. The galvanostatic polarization curves, Tafel curves and anodic polarization curves were tested in sulfuric acid solution. The morphologies and phase compositions of the anodic layers formed after galvanostatic polarization were investigated by using scanning electron microscope (SEM) and X-ray diffractometer (XRD), respectively. The results showed that  $\beta$ -PbO<sub>2</sub> can improve the electrocatalytic activity of anodic oxide. The anode containing 3%  $\beta$ -PbO<sub>2</sub> had the lowest overpotential of oxygen evolution reaction (OER) and the best corrosion resistance. The morphologies of the anode surfaces were gradually transformed from regular crystals to amorphous ones as the content of  $\beta$ -PbO<sub>2</sub> increased in anodes.

**Key words:** power-pressed Pb–Ag–PbO<sub>2</sub> anode; oxygen evolution overpotential; electrochemical properties; zinc electrowinning

### 1 Introduction

Electrowinning has become a very important method for producing zinc by hydrometallurgy in the past few decades [1–3], in which the oxygen evolution reaction (OER) is a significant anodic reaction [4,5]. The cast Pb–(0.3%–1%)Ag anodes are widely used in zinc electrowinning for their available raw materials and stability [6–8]. For the cast Pb–(0.3%–1%)Ag anodes, the addition of Ag can effectively reduce the overpotential of OER, and the produced PbO<sub>2</sub> coating on the anodes exhibits good properties, such as good corrosion resistance to Cl<sup>−</sup>, which can even be eliminated [9]. However, because there are several problems for the cast Pb–Ag anodes in the zinc electrowinning, such as worse corrosion resistance which reduces the service lifetime of the Pb–Ag anodes (only 1–3 a) [10–12], a lot of precious metal Ag particles are consumed [13]. Most important of all, the cast anodes still have high overpotential of OER in zinc electrowinning [14–16], which results in 20%–30% energy wasted during zinc electrowinning [17].

To solve these problems, many alternative anodes

have been put forward, such as Pb-based multi-variant alloy anodes, porous alloy anodes, dimensionally stable anodes (DSAs), polyaniline anodes, and powder-rolled/powder-pressed (PP) anodes. The Pb-based multi-variant alloys have good mechanical properties, but have little reduction to the overpotential of OER [18]. The porous alloy anodes have larger inner surface, which helps lower the overpotential of OER [19]. However, they are not easy to obtain because of the complex preparation process. The anodes with particle coatings, usually RuO<sub>2</sub>, IrO<sub>2</sub>, and MnO<sub>2</sub> [20–22], formed on the Pb matrix show good electrocatalytic properties, but they show poor corrosion resistance and instability [23]. In addition, the preparation process of these anodes is complex. Compared with the cast Pb–Ag anodes, the powder-rolled/powder-pressed anodes show better creep resistance, lower overpotential of OER and better corrosion resistance [24], which are considered to be a more promising candidate for zinc electrolysis.

In our previous work [25], it has been found that the electrochemical performance of PP Pb–0.4%Ag anode is better than that of the cast Pb–0.6%Ag anode. In addition, it is reported that the  $\beta$ -PbO<sub>2</sub> has good corrosion resistance and electrocatalytic properties,

**Foundation item:** Project (2017YFB0305401) supported by the National Key R&D Program of China; Projects (51874369, 51474245, 51871249) supported by the National Natural Science Foundation of China; Project (2018JJ3659) supported by the Natural Science Foundation of Hunan Province, China; Project (2018RS3007) supported by Huxiang Young Talents Plan, China

**Corresponding author:** Tie-chui YUAN; Tel/Fax: +86-731-88830142; E-mail: [tiechuiyuan@csu.edu.cn](mailto:tiechuiyuan@csu.edu.cn)

DOI: 10.1016/S1003-6326(19)65148-4

which could improve the electrochemical properties of the anodes [9]. In order to further study the effect of  $\beta$ -PbO<sub>2</sub> on the performance of anode, in this study, the PP Pb–Ag–PbO<sub>2</sub> composite anodes were prepared with the fixed 0.4% Ag content and various  $\beta$ -PbO<sub>2</sub> contents (1%, 2%, 3%, 4% and 5%, mass fraction). For comparison, the performances of cast Pb–0.6%Ag anode and PP Pb–0.4%Ag anode were also investigated. The electrochemical properties of the anodes were systematically tested. The micromorphologies and phase compositions of the oxide layer after galvanostatic polarization were also studied.

## 2 Experimental

### 2.1 Preparation of sample

The  $\beta$ -PbO<sub>2</sub> powders with particle size <5  $\mu$ m (99.00% purity, Shanghai Macklin Biochemical Co., Ltd., China), Ag powders with particle size <8  $\mu$ m (99.99% purity, Chengdu Lianhe Chemical Pharmaceutical Co., Ltd., China) and Pb powders with particle size <42  $\mu$ m (99.95% purity, Sinopharm Chemical Reagent Co., Ltd., China) were used as raw materials. The XRD pattern and SEM image of the  $\beta$ -PbO<sub>2</sub> powders are shown in Figs. 1 and 2, respectively.

To obtain the uniformly distributed powder particles, the mixture containing 0.4% Ag, different contents (0, 1%, 2%, 3%, 4% and 5%) of  $\beta$ -PbO<sub>2</sub> powder and Pb powders was milled in a plastic tube at a rotating speed of 65 r/min for 48 h in air. The mixture was put into a steel mold and pressed under a pressure of 65 MPa for 5 min. And then, the compacts were sintered at 310 °C for 10 h and a H<sub>2</sub> flow rate of 0.2 L/min under normal pressure. Finally, the sintered samples were cooled to room temperature at a H<sub>2</sub> flow rate of 0.2 L/min. For comparison, the Pb–0.6%Ag anode was also prepared by melt casting method. The process flow diagram of PP anodes and the sketch of the mould are shown in Fig. 3.

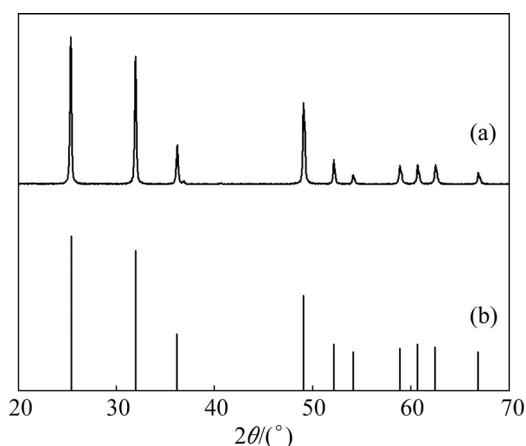


**Fig. 1** XRD patterns of powders: (a) Prepared PbO<sub>2</sub>; (b) Standard  $\beta$ -PbO<sub>2</sub>

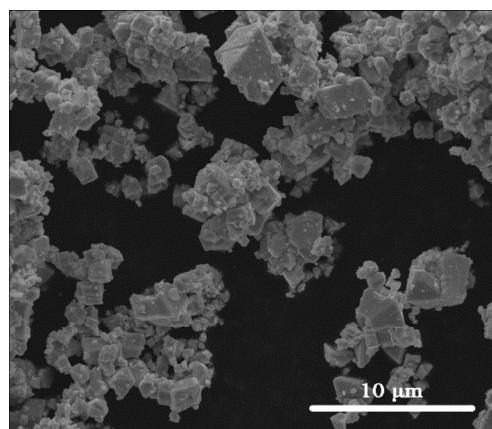


**Fig. 2** SEM image of  $\beta$ -PbO<sub>2</sub> powders

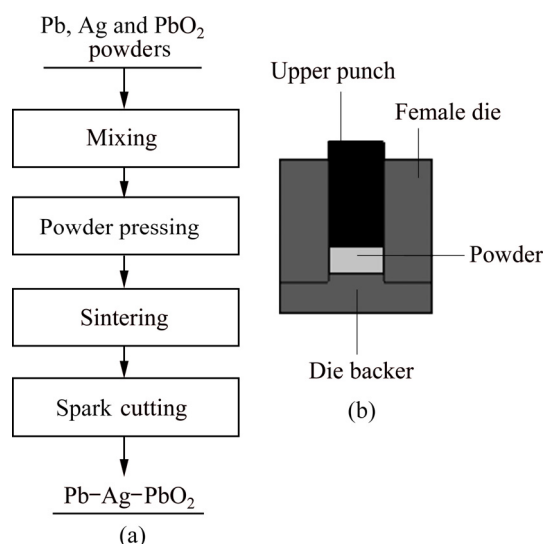


**Fig. 3** Process flow diagram of PP anodes (a) and sketch of mould (b)

### 2.2 Electrochemical measurements

Galvanostatic polarization curves, Tafel curves and anodic polarization curves were obtained with an electrochemical workstation (CHI 760E, Huachen, China) in 500 mL electrolyte solution at 35 °C. The galvanostatic polarization tests were performed in a solution of 160 g/L H<sub>2</sub>SO<sub>4</sub> at a current density of 50 mA/cm<sup>2</sup> for 72 h. The Tafel and anodic polarization tests were done in a solution containing 50 g/L Zn<sup>2+</sup> and 160 g/L H<sub>2</sub>SO<sub>4</sub> after galvanostatic polarization at the scanning rates of 3 and 0.5 mV/s from 1.4 to 1.8 V (vs SCE), respectively. A three-electrode cell was used, in which the reference electrode was a saturated calomel electrode (SCE), the counter electrode was a platinum plate, and the working electrode was the sample with an exposed area of 1.0 cm<sup>2</sup>. The assembly diagram of the anode is shown in Fig. 4.

All the samples were polished with 1500-grit SiC paper before galvanostatic polarization tests, and they

were washed with distilled water and dried with warm air after each electrochemical test.

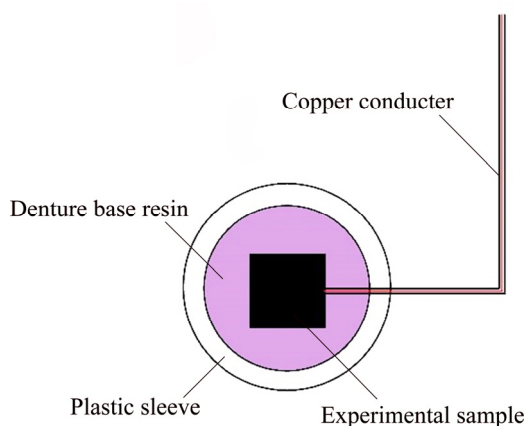


Fig. 4 Sketch diagram of experimental sample

### 2.3 Characterization

The morphologies of the samples after galvanostatic polarization tests of 72 h were observed by SEM (Nova Nano SEM 230). The phases of the oxide layer formed on the anode surface after galvanostatic polarization tests of 72 h were identified by XRD (Rigaku D/MAX-2250) with Cu  $K_{\alpha}$  radiation.

## 3 Result and discussion

### 3.1 Galvanostatic polarization

In order to study the effects of different anodes on the overpotentials of OER, the galvanostatic polarization tests were carried out under a current density of  $50 \text{ mA/cm}^2$  in a solution of  $160 \text{ g/L H}_2\text{SO}_4$  at  $35 \text{ }^\circ\text{C}$  and the results are shown in Fig. 5.

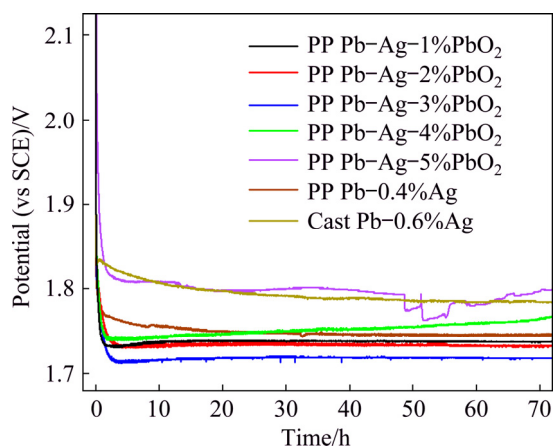


Fig. 5 Galvanostatic polarization curves of different anodes

All the anodes showed different anodic behaviors. At the initial stage of galvanostatic polarization test, the potential of all the anodes dropped dramatically with time, and eventually kept stable except for the PP

Pb-Ag-5%PbO<sub>2</sub> anode. With the continuous formation of oxide layer on the anode surface [22,26,27], the potential of the cast Pb-0.6%Ag anode was stabilized around  $1.79 \text{ V}$  (vs SCE) after 44 h of polarization test. Compared with the cast Pb-0.6%Ag anode, the PP Pb-0.4%Ag anode showed lower stable potential in the galvanostatic polarization test which was around  $1.73 \text{ V}$  (vs SCE) after 44 h, which is consistent with our previous study.

As for the PP Pb-Ag-PbO<sub>2</sub> composite anodes, with the increase of  $\beta$ -PbO<sub>2</sub> content, the potential of anode was firstly decreased and then increased. More specifically, the potentials of PP anodes containing 1%, 2% and 3% PbO<sub>2</sub> were stabilized around  $1.72$ ,  $1.72$  and  $1.71 \text{ V}$  (vs SCE) after 55, 30, and 13 h of polarization tests, respectively. The potential of the anode containing 4% PbO<sub>2</sub> was firstly decreased and then increased, which is obviously distinguished with the other anodes; while, the potential of the anode containing 5% PbO<sub>2</sub> presented obvious fluctuation and was significantly higher than that of the other anodes at the end of the test.

According to Fig. 5, the overpotential of OER decreased with the increase of  $\beta$ -PbO<sub>2</sub> content ( $\leq 3\%$ ) in the anode during the galvanostatic polarization test, which can be explained as follows: (1) OER can be facilitated by  $\beta$ -PbO<sub>2</sub>; (2) the increase of  $\beta$ -PbO<sub>2</sub> content is conducive to the increase of surface area of the anode. However, when the content of  $\beta$ -PbO<sub>2</sub> is higher than 3%, it will have great impact on the mechanical strength of the anode, which is not conducive to the formation of dense oxide layer and can even cause the shedding of the oxide layer. The cracks and loose structures of the oxide layers may be the reasons for the fluctuation of potential.

In conclusion, according to the results shown in Fig. 5, the  $\beta$ -PbO<sub>2</sub> powders ( $\leq 3\%$ ) could improve the electrocatalytic activity of the anodes and the PP Pb-Ag-3%PbO<sub>2</sub> anode showed the lowest overpotential of OER and the best stability among the studied samples, which makes it promising alternative for zinc electrolysis.

### 3.2 Tafel curves

The corrosion resistance of the PP Pb-Ag-PbO<sub>2</sub> composite anodes was evaluated by the Tafel curves obtained in the solution containing  $50 \text{ g/L Zn}^{2+}$  and  $160 \text{ g/L H}_2\text{SO}_4$  under a scanning rate of  $3 \text{ mV/s}$  at  $35 \text{ }^\circ\text{C}$  after galvanostatic polarization. The results are shown in Fig. 6.

Table 1 shows the corrosion potential ( $\varphi_{\text{corr}}$ ) and corrosion current density ( $J_{\text{corr}}$ ), which were obtained by the linear fitting of Tafel curves (Fig. 6). As well known,  $J_{\text{corr}}$  is a kinetic parameter and  $\varphi_{\text{corr}}$  is a thermodynamic parameter, and  $J_{\text{corr}}$  is usually used to evaluate the corrosion resistance of the anode [28]:

$$v = \frac{MJ_{\text{corr}}}{nF} \quad (1)$$

where  $v$  is the corrosion rate,  $n$  is the valence of metal,  $F$  is the Faraday constant, and  $M$  is the mole mass of metal.

As shown in Table 1, compared with the PP Pb–0.4%Ag anode, for all the PP Pb–Ag–PbO<sub>2</sub> composite anodes, the current densities are decreased firstly at  $\beta$ -PbO<sub>2</sub> content  $\leq 3\%$  and then increased at  $\beta$ -PbO<sub>2</sub> content  $> 3\%$ , and the anode containing 3% PbO<sub>2</sub> has the lowest  $J_{\text{corr}}$  ( $3.50 \times 10^{-5}$  A/cm<sup>2</sup>) and  $\varphi_{\text{corr}}$  (–0.338 V), which exhibits the best corrosion resistance. This means that appropriate addition of  $\beta$ -PbO<sub>2</sub> can improve the corrosion resistance of the anode [29], while excessive addition of  $\beta$ -PbO<sub>2</sub> will cause the decrease of corrosion resistance of the anode. The corrosion resistance of the anode is closely related to the morphology of the surface oxide layer.

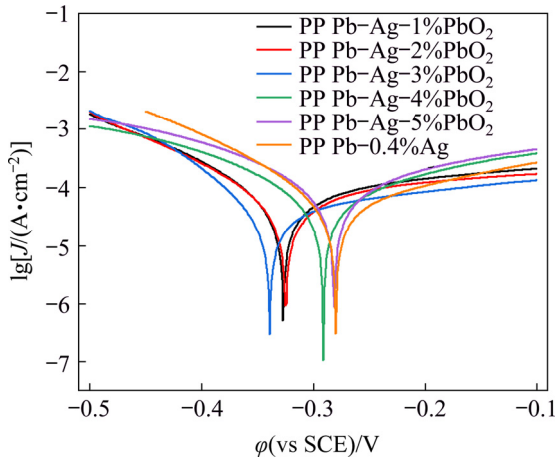


Fig. 6 Tafel curves of different anodes

Table 1 Corrosion potentials and corrosion current densities of different anodes

Anode	$\varphi_{\text{corr}}$ (vs SCE)/V	$J_{\text{corr}}$ (A·cm <sup>-2</sup> )
PP Pb–Ag–1%PbO <sub>2</sub>	–0.327	$6.14 \times 10^{-5}$
PP Pb–Ag–2%PbO <sub>2</sub>	–0.325	$5.30 \times 10^{-5}$
PP Pb–Ag–3%PbO <sub>2</sub>	–0.338	$3.50 \times 10^{-5}$
PP Pb–Ag–4%PbO <sub>2</sub>	–0.291	$6.36 \times 10^{-5}$
PP Pb–Ag–5%PbO <sub>2</sub>	–0.281	$8.57 \times 10^{-5}$
PP Pb–0.4%Ag	–0.298	$6.20 \times 10^{-5}$

### 3.3 Anodic polarization

To study the oxygen evolution behaviors of different anodes after galvanostatic polarization, anodic polarization tests were carried out at a scanning speed of 0.5 mV/s in a solution containing 50 g/L Zn<sup>2+</sup> and 160 g/L H<sub>2</sub>SO<sub>4</sub> at 35 °C, and the results are shown in Fig. 7. The order of oxygen evolution potentials from low to high is: Pb–Ag–3%PbO<sub>2</sub> < Pb–Ag–2%PbO<sub>2</sub> < Pb–Ag–1%PbO<sub>2</sub> < Pb–Ag–4%PbO<sub>2</sub> < Pb–Ag–5%PbO<sub>2</sub>

< Pb–0.4%Ag. This trend is consistent with the final potential of galvanostatic polarization in Fig. 5 and the Pb–Ag–3%PbO<sub>2</sub> anode has the lowest overpotential of OER.

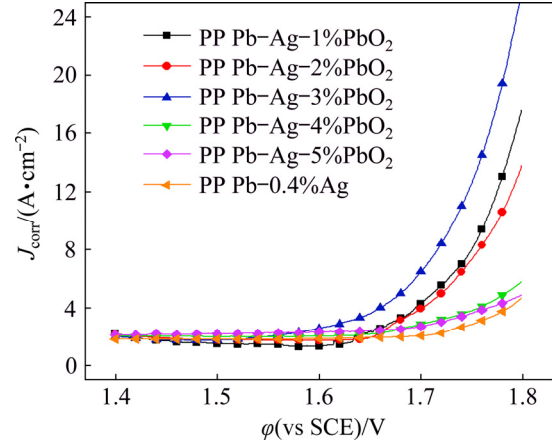


Fig. 7 Anodic polarization curves of different anodes

Table 2 lists the kinetic parameters ( $a$ ,  $b$  and  $J_0$ ) and the overpotential of OER ( $\eta$ ) for all the Pb–Ag–PbO<sub>2</sub> composite anodes obtained at a current density of 50 mA/cm<sup>2</sup>. The value of  $\eta$  is calculated with Eq. (2) [30,31].

$$\eta = \varphi + 0.2373 - 1.260 - JR_s \quad (2)$$

where  $R_s$  is the solution resistance between the working electrode and the reference electrode,  $J$  is the current density corresponding to  $\varphi$ ,  $\varphi$  is the anodic potential, 1.260 is the equilibrium potential of OER, and 0.2373 is the potential of SCE. And then,  $a$ ,  $b$  can be obtained by linear fitting of  $R_s$ -corrected lines ( $\eta - \lg J$ ) according to Eq. (3), and the exchange current density ( $J_0$ ) can also be calculated through Eq. (3) at  $\eta = 0$ .

$$\eta = a + b \lg J \quad (3)$$

From Table 2, it can be seen that the order of  $J_0$  from low to high is: Pb–0.4%Ag < Pb–Ag–5%PbO<sub>2</sub> < Pb–Ag–4%PbO<sub>2</sub> < Pb–Ag–1%PbO<sub>2</sub> < Pb–Ag–2%PbO<sub>2</sub> < Pb–Ag–3%PbO<sub>2</sub>, and the Pb–Ag–3%PbO<sub>2</sub> anode has the highest  $J_0$  value ( $1.02 \times 10^{-5}$  A/cm<sup>2</sup>). We usually

Table 2 Kinetic parameters of oxygen evolution reaction of anodes

Anode	$a$	$b$	$J_0'$ (A·cm <sup>-2</sup> )	$\eta$ (vs SCE)/V
PP Pb–Ag–1%PbO <sub>2</sub>	1.150	0.215	$4.46 \times 10^{-6}$	0.870
PP Pb–Ag–2%PbO <sub>2</sub>	1.120	0.212	$5.27 \times 10^{-6}$	0.844
PP Pb–Ag–3%PbO <sub>2</sub>	1.064	0.213	$1.02 \times 10^{-5}$	0.786
PP Pb–Ag–4%PbO <sub>2</sub>	1.727	0.319	$3.89 \times 10^{-6}$	1.311
PP Pb–Ag–5%PbO <sub>2</sub>	1.774	0.324	$3.31 \times 10^{-6}$	1.353
PP Pb–0.4%Ag	1.791	0.325	$3.08 \times 10^{-6}$	1.368

evaluate the reversibility of electrode reactions and electrode polarization with the value of  $J_0$  [28]. A higher  $J_0$  indicates that the electrode cannot be easily polarized and has higher electrochemical activity and better reversibility [32]. Table 2 also shows that the Pb–Ag–3%PbO<sub>2</sub> anode has the the lowest  $\eta$  value (0.786 V), which means that the anode has the best energy saving property among all the PP Pb–Ag–PbO<sub>2</sub> composite anodes. Therefore, the Pb–Ag–3%PbO<sub>2</sub> anode has the highest electrochemical activity.

### 3.4 Surface morphology

To find out the reason for the difference of electrochemical properties of different anodes, the

morphologies of the anodes after galvanostatic polarization tests were characterized by SEM, as shown in Fig. 8.

For the PP Pb–0.4%Ag anode (Fig. 8(a)), the oxide layers formed on the anode surface were mainly composed of small crystals/particles, on some of which, small cavities could be found. In comparison, when the low amount of  $\beta$ -PbO<sub>2</sub> is introduced (PP Pb–Ag–1%PbO<sub>2</sub>) (Fig. 8(b)), the oxide layer was mainly composed of smaller regular crystals/particles than PP Pb–0.4%Ag anode (Fig. 8(a)) with different sizes and amorphous particles. When the  $\beta$ -PbO<sub>2</sub> content was further increased to 2% (Fig. 8(c)), the particles/crystals became smaller in size and the proportion of amorphous

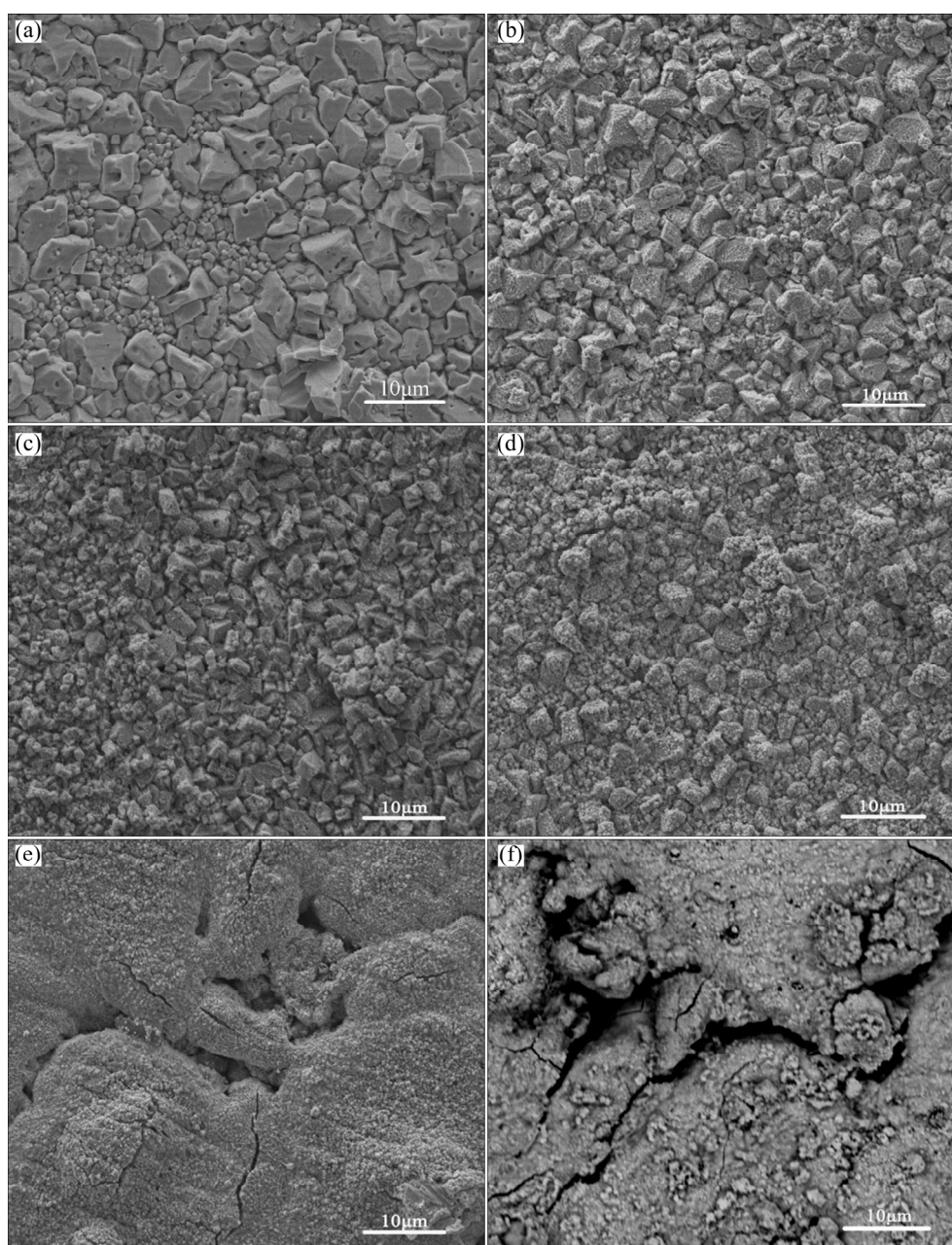


**Fig. 8** SEM images of PP Pb–0.4%Ag (a), PP Pb–Ag–1%PbO<sub>2</sub> (b), PP Pb–Ag–2%PbO<sub>2</sub> (c), PP Pb–Ag–3%PbO<sub>2</sub> (d), PP Pb–Ag–4%PbO<sub>2</sub> (e), and PP Pb–Ag–5%PbO<sub>2</sub> (f)

particles increased significantly. When the  $\beta$ -PbO<sub>2</sub> content was 3% (Fig. 8(d)), the oxide layer was mainly composed of amorphous particles and some regular particles. The results above indicate that the introduction of  $\beta$ -PbO<sub>2</sub> into the PP Pb–0.4%Ag anode is beneficial to the formation of amorphous particles, and the higher content of  $\beta$ -PbO<sub>2</sub> induces the formation of more amorphous particles in the oxide layer. However, when the  $\beta$ -PbO<sub>2</sub> content was increased to 4% (Fig. 8(e)), the oxide layer was composed of amorphous particles and the crystals/particles disappeared, most importantly, some cracks were observed in the oxide layer. With further increase of  $\beta$ -PbO<sub>2</sub> content to 5% (Fig. 8(f)), cracks became significantly larger. The obvious cracks mean that the oxide layer is loose and has weak adhesion, which is easy to fall off during galvanostatic polarization tests. The loose structure and the cracks may be the main reasons for the poor corrosion resistance of PP Pb–Ag–4%PbO<sub>2</sub> and PP Pb–Ag–5%PbO<sub>2</sub> anodes, and are also responsible for the potential fluctuation in the process of galvanostatic polarization test.

### 3.5 Phase analysis

The influence of  $\beta$ -PbO<sub>2</sub> content on the composition and phases of the anodic oxide layer was studied by XRD and the results are shown in Fig. 9.

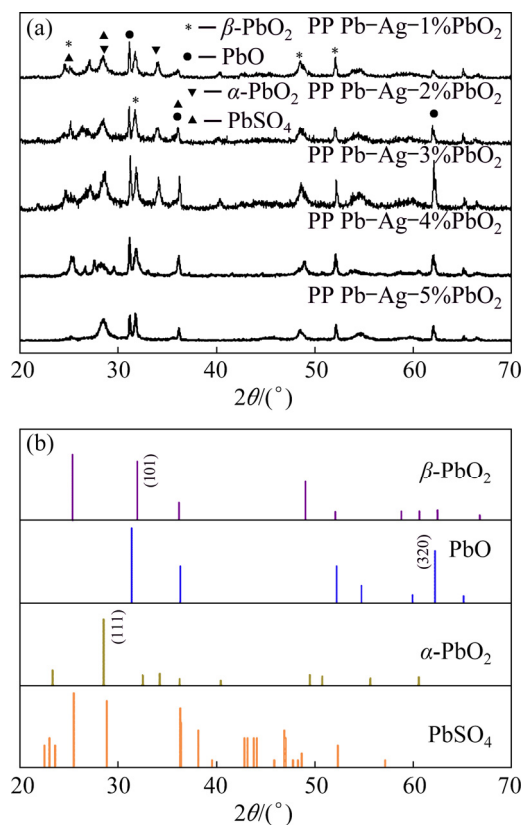


**Fig. 9** XRD patterns of oxide layer of PP anodes after 72 h polarization at 50 mA/cm<sup>2</sup> and 35 °C (a) and diffraction standard cards of  $\beta$ -PbO<sub>2</sub>, PbO,  $\alpha$ -PbO<sub>2</sub> and PbSO<sub>4</sub> (b)

The results showed that for all the Pb–Ag–PbO<sub>2</sub> composite anodes, the oxide layers were mainly composed of PbO,  $\alpha$ -PbO<sub>2</sub>,  $\beta$ -PbO<sub>2</sub>, and PbSO<sub>4</sub>. However, the characteristic absorption peaks of each anode were different. Compared with the anodes containing 4% and 5%  $\beta$ -PbO<sub>2</sub>, the anodes containing 1%, 2% and 3%  $\beta$ -PbO<sub>2</sub> had obvious diffraction peaks of  $\alpha$ -PbO<sub>2</sub> (111). The intensity of the peak of PbO (320) increased with the  $\beta$ -PbO<sub>2</sub> content ( $\leq 3\%$ ), then it decreased when the  $\beta$ -PbO<sub>2</sub> content exceeded 3%. It is worth noting that the increase of  $\beta$ -PbO<sub>2</sub> content in fresh composite anodes had great effect on the intensity of the peak of  $\beta$ -PbO<sub>2</sub> (101) of oxide layers and the changing trend of the absorption peak of  $\beta$ -PbO<sub>2</sub> was consistent with the potential of galvanostatic polarization of Pb–Ag–PbO<sub>2</sub> composite anodes. Therefore, the content of  $\beta$ -PbO<sub>2</sub> in anodes has certain influence on the formation of  $\alpha$ -PbO<sub>2</sub>,  $\beta$ -PbO<sub>2</sub> and PbO. The powder of  $\beta$ -PbO<sub>2</sub> in the anodes may provide some active sites for the formation of transformation of Pb to PbSO<sub>4</sub> and PbSO<sub>4</sub> to  $\beta$ -PbO<sub>2</sub> [29,33]. However, the excessive addition of  $\beta$ -PbO<sub>2</sub> leads to the formation of unstable oxides, which may be the reason for the decline of intensity of PbO.

### 4 Conclusions

(1) As the content of  $\beta$ -PbO<sub>2</sub> increased in the powder-pressed anode, the overpotential of oxygen evolution reaction decreased firstly and then increased. The Pb–Ag–3%PbO<sub>2</sub> anode had the lowest potential.

(2) The addition of an appropriate amount of  $\beta$ -PbO<sub>2</sub> can improve the corrosion resistance of the powder-pressed anodes. The Pb–Ag–3%PbO<sub>2</sub> anode showed the best corrosion resistance.

(3) With increasing the content of  $\beta$ -PbO<sub>2</sub>, the morphologies of the oxide layer changed from regular crystals/particles to amorphous particles. However, excessive addition of  $\beta$ -PbO<sub>2</sub> in the anodes was not conducive to the formation of a highly adhesive oxide layer.

### References

- [1] SOROUR N, ZHANG W, GABRA G, GHALI E, HOULACHI G. Electrochemical studies of ionic liquid additives during the zinc electrowinning process [J]. Hydrometallurgy, 2015, 157: 261–269.
- [2] ZHANG Qi-bo, HUA Xin-yi. Stability of [BMIM] H<sub>2</sub>SO<sub>4</sub> for using as additive during zinc electrowinning from acidic sulfate solution [J]. Journal of Central South University, 2012, 19: 2451–2457.
- [3] ZHANG Chen-mu, DUAN Ning, JIANG Lin-hua, XU Fu-yuan. The impact mechanism of Mn<sup>2+</sup> ions on oxygen evolution reaction in zinc sulfate electrolyte [J]. Journal of Electroanalytical Chemistry, 2018, 811: 53–61.
- [4] KARBASI M, ESKANDAR K A, ELAHEH A D. Electrochemical performance of Pb–Co composite anode during zinc electrowinning

- [J]. Hydrometallurgy, 2018, 183: 51–59.
- [5] CHEN Bu-ming, WANG Shi-chuan, LIU Jian-hua, HUANG Hui, DONG Can-sheng, HE Ya-peng, YAN Wen-kai, GUO Zhong-cheng, XU Rui-dong, YANG Hai-tao. Corrosion resistance mechanism of a novel porous Ti/Sn-Sb-RuO<sub>2</sub>/β-PbO<sub>2</sub> anode for zinc electrowinning [J]. Corrosion Science, 2018, 144: 136–144.
- [6] ZHONG Xiao-cong, JIANG Liang-xing, LIU Fang-yang, LI Jie, LIU Ye-xiang. Anodic passivation of Pb-Ag-Nd anode in fluoride-containing H<sub>2</sub>SO<sub>4</sub> solution [J]. Journal of Central South University, 2015, 22: 2894–2901.
- [7] ZHOU Xiang-yang, WANG Shuai, YANG Juan, GUO Zhong-cheng, YANG Jian, MA Chi-yuan, CHEN Bu-ming. Effect of cooling ways on properties of Al/Pb-0.2%Ag rolled alloy for zinc electrowinning [J]. Transactions of Nonferrous Metals Society of China, 2017, 27: 2096–2103.
- [8] ZHANG Cheng, LIU Jian-hua, CHEN Bu-ming. Effect of CeO<sub>2</sub> and graphite powder on the electrochemical performance of Ti/PbO<sub>2</sub> anode for zinc electrowinning [J]. Ceramics International, 2018, 44: 19735–19742.
- [9] YANG Hai-tao, CHEN Bu-ming, GUO Zhong-cheng, LIU Huan-rong, ZHANG Yong-chun, HUANG Hui, XU Rui-dong, FU Ren-chun. Anodic behavior and microstructure of Al/Pb-Ag-Co anode during zinc electrowinning [J]. Transactions of Nonferrous Metals Society of China, 2014, 24: 3394–3404.
- [10] XU R D, HUANG L P, ZHOU J F, ZHAN P, GUAN Y Y, KONG Y. Effects of tungsten carbide on electrochemical properties and microstructural features of Al/Pb-PANI-WC composite inert anodes used in zinc electrowinning [J]. Hydrometallurgy, 2012, 125: 8–15.
- [11] ZHONG Xiao-cong, YU Xiao-ying, LIU Zheng-wei, JIANG Liang-xing, LI Jie, LIU Ye-xiang. Comparison of corrosion and oxygen evolution behaviors between cast and rolled Pb-Ag-Nd anodes [J]. International Journal of Minerals, Metallurgy and Materials, 2015, 22: 1067–1075.
- [12] XIA X L, ZHITOMIRSKY I, MCDERMID J R. Electrodeposition of zinc and composite zinc-yttria stabilized zirconia coatings [J]. Journal of Materials Processing Technology, 2009, 209: 2632–2640.
- [13] PENG Bing, PENG Ning, LIU Hui, XUE Ke, LIN Dong-hong. Comprehensive recovery of Fe, Zn, Ag and in from high iron-bearing zinc calcine [J]. Journal of Central South University, 2017, 24: 1082–1089.
- [14] SOROUR N, SU C, GHALI E, HOULACHI G. Effect of ionic liquid additives on oxygen evolution reaction and corrosion behavior of Pb-Ag anode in zinc electrowinning [J]. Electrochimica Acta, 2017, 258: 631–638.
- [15] LAFRONT A M, ZHANG W, GHALI E, HOULACHI G. Electrochemical noise studies of the corrosion behaviour of lead anodes during zinc electrowinning maintenance [J]. Electrochimica Acta, 2010, 55: 6665–6675.
- [16] CHEN Bu-ming, YAN Wen-kai, HE Ya-peng, HUANG Hui, LENG He, GUO Zhong-cheng, LIU Jian-hua. Influence of F-doped beta-PbO<sub>2</sub> conductive ceramic layer on the anodic behavior of 3D Al/Sn rod Pb-0.75% Ag for zinc electrowinning [J]. Journal of the Electrochemical Society, 2019, 166: E119–E128.
- [17] JAIMES R, MIRANDA-HERNANDEZ M, LARTUNDO-ROJAS L, GONZALEZ I. Characterization of anodic deposits formed on Pb-Ag electrodes during electrolysis in mimic zinc electrowinning solutions with different concentrations of Mn(II) [J]. Hydrometallurgy, 2015, 156: 53–62.
- [18] WANG Wen-jun, WANG Zhuo-ran, YUAN Tie-chui, LI Rui-di, LI Hai-hua, LIN Wen-jun. Oxygen evolution and corrosion behavior of Pb-CeO<sub>2</sub> anodes in sulfuric acid solution [J]. Hydrometallurgy, 2019, 183: 221–229.
- [19] LAI Yuan-qing, JIANG Liang-xing, LI Jie, ZHONG Shui-ping, LÜ Xiao-juan, PENG Hong-jian, LIU Ye-xiang. A novel porous Pb-Ag anode for energy-saving in zinc electrowinning. Part II: Preparation and pilot plant tests of large size anode [J]. Hydrometallurgy, 2010, 102: 81–86.
- [20] ZHANG W, ROBICHAUD M, GHALI E, HOULACHI G. Electrochemical behavior of mesh and plate oxide coated anodes during zinc electrowinning [J]. Transactions of Nonferrous Metals Society of China, 2016, 26: 589–598.
- [21] BARUFFALDI C, CATTARIN S, MUSIANI M. Deposition of non-stoichiometric tungsten oxides + MO<sub>2</sub> composites (M=Ru or Ir) and study of their catalytic properties in hydrogen or oxygen evolution reactions [J]. Electrochimica Acta, 2003, 48: 3921–3927.
- [22] MOHAMMADI M, ALFANTAZI A. Anodic behavior and corrosion resistance of the Pb-MnO<sub>2</sub> composite anodes for metal electrowinning [J]. Journal of the Electrochemical Society, 2013, 160: C253–C261.
- [23] CHEN Bu-ming, GUO Zhong-cheng, YANG Xian-wan, CAO Yuan-dong. Effect of the current density on electrodepositing alpha-lead dioxide coating on aluminum substrate [J]. Acta Metallurgica Sinica (English Letters), 2009, 22: 373–382.
- [24] WANG Shuai, ZHOU Xiang-yang, MA Chi-yuan, LONG Bo, WANG Hui, TANG Jing-jing, YANG Juan. Electrochemical properties of Pb-0.6wt%Ag powder-pressed alloy in sulfuric acid electrolyte containing Cl<sup>-</sup>/Mn<sup>2+</sup> ions [J]. Hydrometallurgy, 2018, 177: 218–226.
- [25] WANG Wen-jun, YUAN Tie-chui, LI Rui-di, WANG Zhuo-ran, LI Hai-hua, LI Lan-bo, ZHENG Dan. Electrochemical behaviors of powder-processed Pb-Ag anodes [J]. The Journal of the Minerals, Metals & Materials Society, 2019, 71: 2498–2504.
- [26] MA Rui-xin, CHENG Shi-yao, ZHANG Xiao-yong, LI Shi-na, LIU Zi-lin, LI Xiang. Oxygen evolution and corrosion behavior of low-MnO<sub>2</sub>-content Pb-MnO<sub>2</sub> composite anodes for metal electrowinning [J]. Hydrometallurgy, 2016, 159: 6–11.
- [27] REROLLE C, WIART R. Kinetics of oxygen evolution on Pb and Pb-Ag anodes during zinc electrowinning [J]. Electrochim Acta, 1996, 41: 1063–1069.
- [28] ZHANG Yong-chun, CHEN Bu-ming, YANG Hai-tao, HUANG Hui, GUO Zhong-cheng. Anodic behavior and microstructure of Al/Pb-Ag-Co anode during zinc electrowinning [J]. Journal of Central South University, 2014, 21: 83–88.
- [29] LAI Yang-qing, LI Yuan, JIANG Liang-xing, LV Xiao-juan, LI Jie, LIU Ye-xiang. Electrochemical behaviors of co-deposited Pb/Pb-MnO<sub>2</sub> composite anode in sulfuric acid solution—Tafel and EIS investigations [J]. Journal of Electroanalytical Chemistry, 2012, 671: 16–23.
- [30] MOHAMMADI M, MOHAMMADI F, HOULACHI G, ALFANTAZI A. The role of electrolyte hydrodynamic properties on the performance of lead-based anodes in electrometallurgical processes [J]. Journal of the Electrochemical Society, 2013, 160: E27–E33.
- [31] WANG Wen-jun, WANG Zhuo-ran, YUAN Tie-chui, LI Rui-di, LI Hai-hua, LIN Wen-jun, ZHENG Dan. Oxygen evolution and corrosion behavior of Pb-CeO<sub>2</sub> anodes in sulfuric acid solution [J]. Hydrometallurgy, 2019, 183: 221–229.
- [32] WANG Wen-jun, YUAN Tie-chui, LI Rui-di, ZHU Xian-yun, LI Hai-hua, LIN Wen-jun, LI Lan-bo, ZHENG Dan. Electrochemical corrosion behaviors of Pb-Ag anodes by electric current pulse assisted casting [J]. Journal of Electroanalytical Chemistry, 2019, 847: 113250.
- [33] HO J C K, FILHO G T, SIMPRAGA R, CONWAY B E. Structure influence on electrocatalysis and adsorption of intermediates in the anodic O<sub>2</sub> evolution at dimorphic α- and β-PbO<sub>2</sub> [J]. Journal of Electroanalytical Chemistry, 1994, 366: 147–162.

## 粉末压制 Pb–Ag–PbO<sub>2</sub> 阳极的电化学性能

李海华<sup>1</sup>, 袁铁锤<sup>1</sup>, 李瑞迪<sup>1</sup>, 王文军<sup>1,2</sup>, 郑 聃<sup>1</sup>, 袁继维<sup>3</sup>

1. 中南大学 粉末冶金国家重点实验室, 长沙 410083;
2. 株洲冶炼集团股份有限公司, 株洲 412004;
3. 贵州省钛材料研发中心有限公司, 遵义 563004

**摘 要:** 采用粉末压制方法制备 Pb–Ag–PbO<sub>2</sub> 阳极, 其中,  $\beta$ -PbO<sub>2</sub> 的质量分数分别为 1%, 2%, 3%, 4%和 5%。在硫酸电解液中测试恒电流极化、塔菲尔和阳极极化曲线。采用扫描电镜(SEM)和 X 射线衍射仪分别观察和测试恒电流极化后阳极表面的形貌和相成分。研究表明,  $\beta$ -PbO<sub>2</sub> 能提高阳极表面氧化层的电催化活性; 含 3%  $\beta$ -PbO<sub>2</sub>(质量分数)的阳极具有最低的析氧过电位和最好的抗腐蚀性能; 随着  $\beta$ -PbO<sub>2</sub> 含量的增加, 阳极表面的形貌从规则晶体转变到无定型状态。

**关键词:** 粉末压制 Pb–Ag–PbO<sub>2</sub> 阳极; 析氧过电位; 电化学性能; 锌电泳

(Edited by Wei-ping CHEN)